2018 EAGE ANNUAL
80TH CONFERENCE + EXHIBITION
COPENHAGEN | DENMARK

Th A12 04

# A Practical Workflow of Full Waveform Inversion to Process Land Seismic Data: Synthetic Study

W. He* (University Grenoble Alpes), R. Brossier (University Grenoble Alpes), L. Metivier (Univ. Grenoble Alpes - CNRS, LJK, University Grenoble Alpes), J. Virieux (University Grenoble Alpes)

## Summary

Designing successful applications of elastic full waveform inversion to 3D land seismic data is challenging. As a preliminary step to investigate such a difficult topic, a realistic target extracted from the SEAM II Foothill benchmark is considered. In such environments with complex near surface (topography and complex near surface properties), three main difficulties are faced: complex and energetic surface-wave masking body waves, unknown source wavelet, and potential trade-offs between multiple parameters describing the subsurface mechanical properties. In this study, we focus on the two first of these difficulties. Relying on the spectral element modeling and inversion code SEM46, we implement an automatic workflow based on a hierarchical data separation designed to introduce surface waves in a later step in the inversion process. We also implement an efficient time-domain source-wavelet estimation allowing to update the source estimation at each iteration of the inversion at almost no cost. These two ingredients make possible the successful reconstruction of both P-wave and S-wave velocity models for the target we consider.

## Introduction

Land seismic full waveform inversion (FWI) is characterised by three challenges: (1) relatively weak body waves, (2) unknown source wavelet and heterogeneous coupling of sources and receivers, and (3) multi-parameter imprint in the data. Land seismic records are generally quite complicated with strong imprints of the topography and the superficial complex geology. Body waves propagating inside the whole medium are often weak compared to surface waves which propagate inside the shallow area. Moreover, variations in topography and/or strong superficial heterogeneities induce significant scattering phases which are difficult to interpret. For overcoming possible ambiguities in the medium reconstruction, progressive frequency content is introduced in the FWI for imaging the medium (Bunks et al., 1995). Low-pass filtering the data enlarges the basin of the objective function, which could possibly avoid any cycle-skipping issues. However, this inversion strategy does not resolve the tradeoff between source wavelets and model parameters.

This study aims to build an automatic workflow to simultaneously update the source wavelets and the model parameters at each iteration. The first two challenges of land seismic FWI will be covered. For doing so, we rely on the 3D visco-elastic modeling and inversion frame (SEM46 code) presented in Trinh et al. (2017a). A spectral element method is implemented as an efficient modeling tool for accurate free surface conditions (Komatitsch and Tromp, 1999). To prevent the surface waves from directing the inversion to local minimum, a crude time window would be used to select the weak body waves at the first step. For the second challenge, the estimation of the source wavelet could be achieved by integrating source unknowns in the optimization corresponding to a deconvolution (Pratt, 1999) or through an independent optimization (Plessix and Cao, 2011) corresponding to a matching filter. The first way estimates the source wavelet first and then re-starts the program to calculate the gradient and update the model. There are totally four forward simulations at each iteration (one for the source estimation and three for the gradient calculation). To save the computation time, the source estimation is usually conducted every few iterations. The second way estimates the source wavelet on the fly at each iteration: negligible extra computation is observed practically. In this study, we directly implement this last option in the time-domain FWI process. Although multi-parameters reconstruction including anisotropy will be the long-term objective of this research, only velocity parameters (P- and S-wave velocity) are taken as unknowns in the present workflow design.

## Method: matching filter

*Theory: source estimation*

A matching filter is a function which transfers synthetics onto the observed data. Estimating the matching filter could be cast as an optimization problem through the least-squares misfit

$$\begin{aligned} J &= \tfrac{1}{2}\textstyle\sum_{r,s}\int_0^T \mathrm{d}t\left[\left(\int_0^T \mathrm{d}\tau p(t-\tau)w(\tau)\right)-d(t)\right]^2 \mathscr{W}(t) \\ &= \tfrac{1}{2} < conv(p,w)-d|\mathscr{W}|conv(p,w)-d >, \end{aligned} \tag{1}$$

with the compact Dirac bra-ket notation for the inner product, the convolution denoted by *conv* and a summation over sources and receivers. The synthetics are denoted by $p(t)$ and observed data by $d(t)$. The source frequency band for synthetics should be broader than the one for data. The inner product is defined as an integral over recorded time window $[0,T]$ with a weight $\mathscr{W}$. In following numerical experiments, it will be simply zero for near-offset traces and one for all other traces. We suggest to include all the waves to estimate the source wavelet; adding a time window usually leads to distorted source wavelets. For each corresponding trace $(p(t),d(t))$, there exists a matching filter $w(t)$. However, one may assume that all shots share the same wavelet and an optimal matching filter is obtained by zeroing the first-order perturbation

$$\delta J = < conv(p,\delta w)|\mathscr{W}|conv(p,w)-d > = < \delta w|xcorr(p,\mathscr{W}conv(p,w)-\mathscr{W}d) > = 0, \tag{2}$$

where the cross-correlation between two signals is denoted by *xcorr*. The matching-filter solution will be given by solving the equation

$$\sum_{r,s} xcorr(p, \mathscr{W} conv(p,w) - \mathscr{W} d) = 0 : \quad \sum_{r,s} xcorr(p, \mathscr{W} conv(p,w)) = \sum_{r,s} xcorr(p, \mathscr{W} d) \tag{3}$$

In this study, we simulate the synthetic $p(t)$ with a $\delta(t)$ function; then the matching filter $w(t)$ turns out to be the estimated source wavelet.

*Theory: adjoint source for model parameter updating*

The objective function being used to produce the misfit gradient for updating model parameters could be different from the one being used to estimate the source wavelet (Plessix and Cao, 2011). In this study, we simply consider the least-squares objective function shown in Equation (1), but with a different weighting function $\mathscr{W}_m$. In a first step of the inversion, it includes a time window for muting surface waves. In the second step, this time window is removed. Knowing the matching filter $w$, the adjoint source is obtained by looking at the first-order perturbation of the objective function.

$$\delta J = < conv(\delta p, w) | \mathscr{W}_m | conv(p,w) - d > = < \delta p | xcorr(w, \mathscr{W}_m conv(p,w) - \mathscr{W}_m d) > . \tag{4}$$

Incorporating inside a FWI workflow the matching filter deduced from the source estimation does not imply much algorithmic modification, except the adjoint source when computing the adjoint field.

**Synthetic 3D elastic FWI experiments**

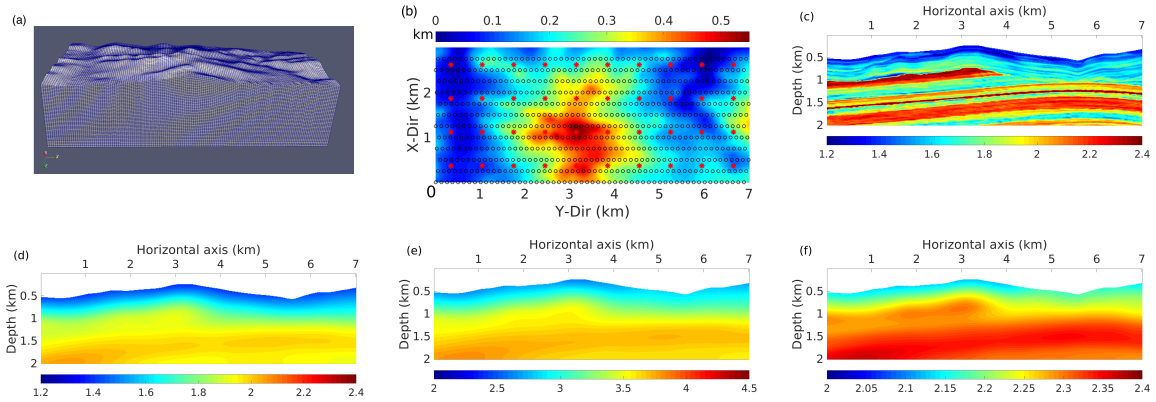


***Figure 1*** *(a) the 3D mesh, (b) acquisition (red dots are sources and black circles receivers), (c) the true $v_s$ velocity, (d) the initial $v_s$ velocity, (e) the initial $v_p$ velocity and (f) the initial/true density $\rho$.*

A modified version of the SEAM Phase II Foothill model is considered, increasing slightly the velocity of the very-shallow sediment layer (Figure 1c). We select an area of $3 \times 7 \times 2\,\mathrm{km}^3$ in the $x$, $y$, and $z$ directions. The initial velocity model is obtained by smoothing the true model with a 1 km long 3D filter (Figure 1d). The fixed density is obtained by smoothing the true density with a 800 m long 3D filter. Fine scale structures disappear in initial models.

The observed data are generated with a fine mesh with an element size of 50 m in each direction (Figure 1a). The source wavelet is a 6 Hz Ricker wavelet, and the time interval is 0.3 ms. Fourty vertical forces are used (Figure 1b). Three component receivers are equidistantly distributed every 12.5 m in $x$ direction and 25 m in $y$ direction. After the simulation, the 6 Hz Ricker wavelet is deconvolved from the seismic data, which means that observed data have a flat spectrum which is bandpassed in the range from 2 Hz to 3.5 Hz (Figure 2a). This band-limited data are taken as the observed data that we used to test our workflow.

For the inversion, the mesh size is enlarged to 100 m, and the time interval is increased to 0.6 ms. The initial guess of the wavelet is a delta function. The estimated matching filter (Equation (3)) is injected

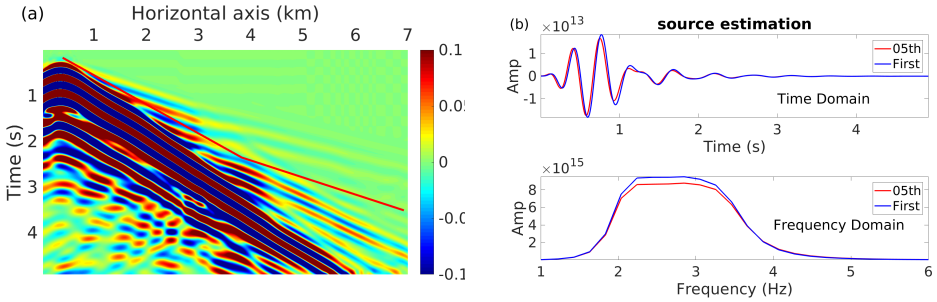


***Figure 2*** *(a) Observed $v_z$ component, frequency range is $[2, 3.5]$ Hz. (b) Estimated source wavelets in time/frequency domain at first/last iteration of the first step inversion are not too far from a box window.*

into the adjoint source by Equation (4). The gradient is classicaly obtained by zero-lag cross-correlation of the adjoint wavefield and the rebuilt incident wavefield at the same time. Gradient is smoothed using Bessel filters (Trinh et al., 2017b) for removing numerical artifacts. A depth pre-conditioner, given by the expression $(z+100)^2$ with the depth $z$ in meters, is applied to compensate geometrical spreading effects of the gradient at depth. After these evaluations, the model is updated following a line search with a quasi-Newton optimisation method L-BFGS (Nocedal and Wright, 2006).

The inversion is separated into two steps: the first considers only body waves while the second takes into account all waves. In the first step, we manually designed a crude time window by looking at the observed data. The time window aggressively mutes the surface waves and the scattered waves (red line in Figure 2a). The model is updated for five iterations before reaching a maximum line search number. The estimated source wavelet is not too far away from the box window between 2 Hz to 3.5 Hz, even at the first iteration: only small variations in amplitude and phase are observed at the fifth iteration(Figure 2b). The smoothed gradient, the preconditioned one and the inverted model are shown in the top row of Figure 3. Compared to the initial velocity (Figure 1d), the inverted velocity (Figure 3c1) shows long-wavelength structures. Then, the time window is removed such that all waves are now included to the inversion. The initial model of the second step is the final model of the first step. There are 35 iterations in this second step, and the relative misfit decreases to 24%. The filtered gradient, the preconditioned one and the inverted model are shown in the bottom row of Figure 3: the final model shows improved finer-scale structures. Figure 5 shows initial, inverted, true and filtered true models at the second step for different vertical profiles for more quantitative analysis.

The inversion is a multi-parameter inversion, and the inverted P-wave velociy $v_p$ is shown in Figure 4. The main features of $v_p$ is recovered during the first step when body waves are only used. The velocity $v_p$ is not much updated during the second step mainly because the dominant surface waves are much less sensitive to the $v_p$ parameter than to the $v_s$ parameter.

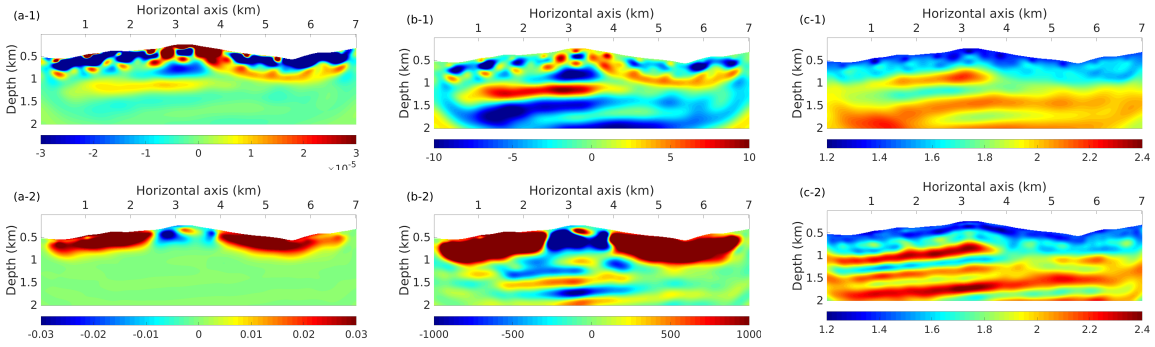


***Figure 3*** *In the first step where only the body waves are selected, (a-1) initial $v_s$-gradient, (b-1) the preconditioned initial $v_s$-gradient, (c-1) the inverted $v_s$. In the second step with all the waves, (a-2) initial $v_s$-gradient, (b-2) the preconditioned initial $v_s$-gradient, (c-2) the inverted $v_s$.*

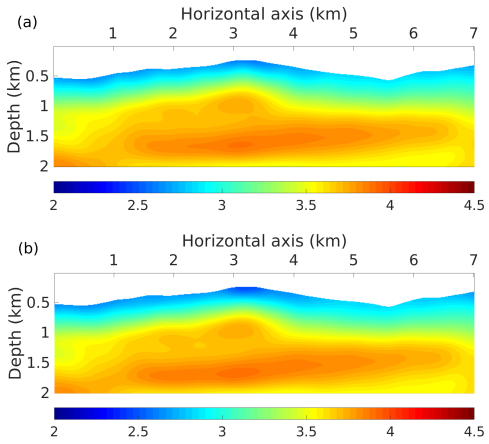


***Figure 4*** *Inverted $v_p$ at the (a) first and (b) second step.*

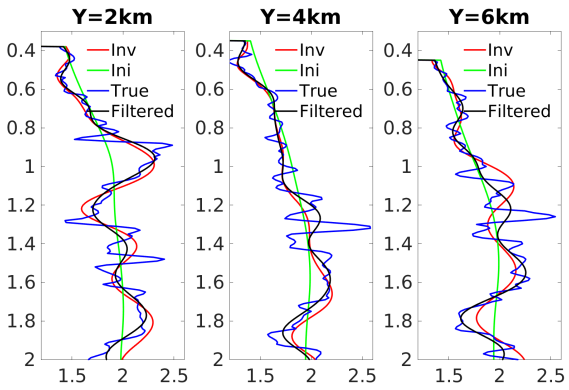


***Figure 5*** *Comparison of $v_s$ velocity vertical profiles at three positions in Figure 3. The label* Filtered *corresponds to the filtered true model in the frequency rang* $[2, 3.5]$ *Hz.*

## Conclusion

A practical workflow of elastic FWI has been designed for handling land seismic data. The observed data, which are computed on a different mesh used for the inversion, are processed in such a way (deconvolution and band-pass filter) that the actual source wavelet micmics a box window. In an alternative way, we apply a matching filter technique to update the source wavelet and the least-squares misfit function for updating the model parameters. The inversion is performed in a hierarchical way: the first step involves body waves by using an aggressive time window, and the second one consider both body and surface waves. The final model shows relatively fine-scale structures as expected and the source signal is accurately deduced.

## Acknowledgements

This study was partially funded by the SEISCOPE consortium (*http://seiscope2.osug.fr*), sponsored by AKERBP, CGG, CHEVRON, EXXON-MOBIL, JGI, PETROBRAS, SCHLUMBERGER, SHELL, SINOPEC, STATOIL and TOTAL. This study was granted access to the HPC resources of SIGAMM infrastructure (http://crimson.oca.eu) and CINES/IDRIS/TGCC under the allocation 046091 made by GENCI.

## References

Bunks, C., Salek, F.M., Zaleski, S. and Chavent, G. [1995] Multiscale seismic waveform inversion. *Geophysics*, **60**(5), 1457–1473.

Komatitsch, D. and Tromp, J. [1999] Introduction to the spectral element method for 3D seismic wave propagation. *Geophysical Journal International*, **139**, 806–822.

Nocedal, J. and Wright, S.J. [2006] *Numerical Optimization*. Springer, 2nd edn.

Plessix, R.E. and Cao, Q. [2011] A parametrization study for surface seismic full waveform inversion in an acoustic vertical transversely isotropic medium. *Geophysical Journal International*, **185**, 539–556.

Pratt, R.G. [1999] Seismic waveform inversion in the frequency domain, part I : theory and verification in a physical scale model. *Geophysics*, **64**, 888–901.

Trinh, P.T., Brossier, R., Métivier, L., Tavard, L. and Virieux, J. [2017a] Efficient 3D elastic FWI using a spectral-element method. In: *87th SEG Conference and Exhibition 2017, Houston*.

Trinh, P.T., Brossier, R., Métivier, L., Virieux, J. and Wellington, P. [2017b] Bessel smoothing filter for spectral element mesh. *Geophysical Journal International*, **209**(3), 1489–1512.